

Effect of Cyano Substituents on Electron Affinity and Electron-Transporting Properties of Conjugated Polymers

Michelle S. Liu, Xuezhong Jiang, Sen Liu, Petra Herguth, and Alex K.-Y. Jen*

Department of Materials Science and Engineering, Box 352120, University of Washington, Seattle, Washington 98195-2120

Received October 15, 2001; Revised Manuscript Received February 1, 2002

ABSTRACT: A series of cyano-containing distyrylbenzenes were synthesized as the model compounds to systematically study the effect of cyano substituents on the redox behaviors of conjugated molecules. By introducing the electron-withdrawing functional groups (cyano and dicyanovinyl) onto the phenylene ring, both electron affinity and electrochemical stability of the resulting distyrylbenzenes are greatly enhanced. The results enabled us to design and synthesize a new class of highly electron affinitive, fluorene-based copolymers with these cyano-containing chromophores as comonomers. The effects of acceptor strength and side chain on electron-transporting properties of these polymers were also investigated. By properly adjusting copolymer compositions, a combined high electron affinity and transport was achieved in a statistic copolymer, poly(fluorenebenzothiadiazole–cyanophenylenevinylene) (PFB–CNPV). An external quantum efficiency up to 0.88% and brightness as high as 4730 cd/m² were achieved in a double-layer light-emitting diode (LED) using PFB–CNPV as the emitting layer.

Introduction

Conjugated polymers with excellent luminescent properties are very attractive for indicator and flat-panel display applications due to their low cost, convenient processability, and ease to fine-tune the emission colors. A wide range of polymers, poly(*p*-phenylenevinylene) (PPV), polythiophene (PT), poly(*p*-phenylene) (PPP), polyfluorene (PF), and their derivatives, have been extensively investigated as emissive materials.^{1–3} Electroluminescence (EL) in these materials is usually achieved by injecting electrons from a cathode into the conduction band and holes from an indium tin oxide (ITO) anode into the valence band of the polymers. These injected holes and electrons capture each other to form excitons, whose radiative decay emits light. A balanced charge injection from both electrodes and comparable mobility of electrons and holes within the polymers are crucial to achieve high device efficiency.

However, most of the conjugated polymers tend to possess low electron affinity.¹ In addition, electron transport is often reduced by the presence of defect- and impurity-related traps in polymer films, while these defects and impurities show little effect on the hole transport. For these reasons, the majority of the charge carriers in these emissive polymers are usually holes, owing to their smaller injection barriers and higher mobilities.^{4,5} Although electron injection can be facilitated by using low work function metals as cathode (such as calcium or magnesium), the low electron mobility in polymer still results in unbalanced charge transport.^{6,7} As a result, the improvement of EL efficiency is quite limited. Therefore, it is a major challenge to find suitable conjugated polymers that possess enhanced electron injection and transport simultaneously.

The optoelectronic properties of a conjugated polymer are primarily governed by the chemical structure of the polymer backbone. By choosing suitable functional groups attached onto the polymer main chain, it is

possible to fine-tune the highest occupied molecular orbital (HOMO) and the lowest unoccupied molecular orbital (LUMO) energy levels and alter its electronic properties. These properties will eventually affect the charge transport characteristics of the materials.^{8–10} Previously, the results from a processable poly(cyano-terephthalylidene) (CN–PPV), a dialkoxy-substituted PPV derivative with cyano groups on the vinylene units, have demonstrated a high internal quantum efficiency up to 4% in a double-layer device (ITO/PPV/CN–PPV/Al).¹¹ This improved device efficiency was attributed to better electron injection facilitated by the electron-withdrawing cyano groups. However, the CN–PPV was synthesized by using the Knoevenagel condensation polymerization. A careful control over reaction conditions is required to avoid the Michael addition side reactions that will cause cross-linking and lead to polymers with inferior EL properties. In this paper, a series of cyano-containing distyrylbenzenes (**3–6**) with electron-withdrawing groups functionalized on the phenylene ring were synthesized initially as the model compounds to study the effect of substituents on the electrochemical properties of these oligomers. This was achieved through a systematic changing of acceptor strength on the aromatic ring (Chart 1). The data obtained on these molecular models were used to predict the ultimate electronic and electrochemical properties of an ideal defect-free polymer chain. Based on this model study, a series of light-emitting copolymers with these cyano-containing chromophores as building blocks were synthesized, and their electron affinity and charge-transporting properties were investigated (Chart 2).

Experimental Section

Materials. Commercially available chemicals (Aldrich) were used without further purification. 2,5-Dicyano-*p*-xylyl-bis-(diethylphosphonate),^{12,13} 9,9-dihexylfluorene-2,7-di(ethylenyl boronate),¹⁴ 2,5-dibromoterephthalaldehyde,¹⁵ 4-bromo-2,5-dioctylbenzaldehyde,¹⁶ 4,7-dibromo-2,1,3-benzothiadiazole,¹⁷ and 1,4-bis(4-bromostyryl)-2,5-dicyanobenzene¹⁸ were prepared according to the procedures from the literature. All reactions were performed under a dry nitrogen atmosphere.

* To whom correspondence should be addressed.

Chart 1. Chemical Structure of Cyano-Containing Model Compounds

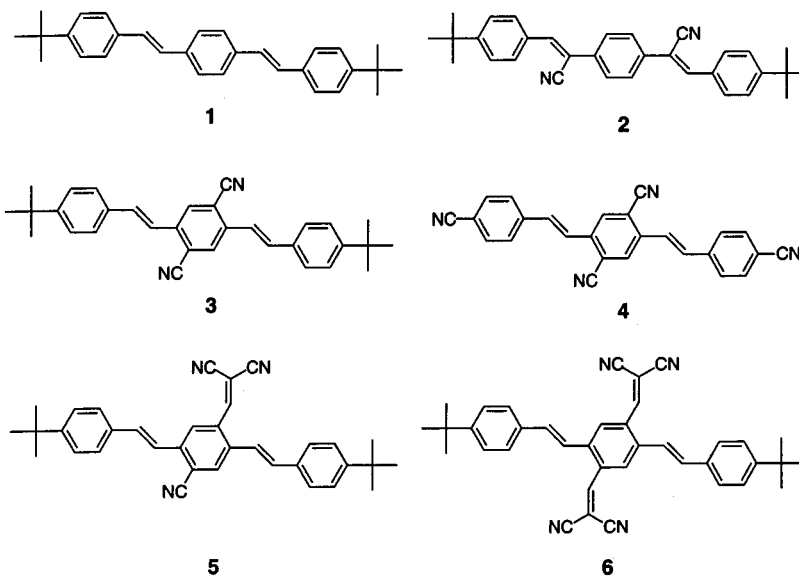
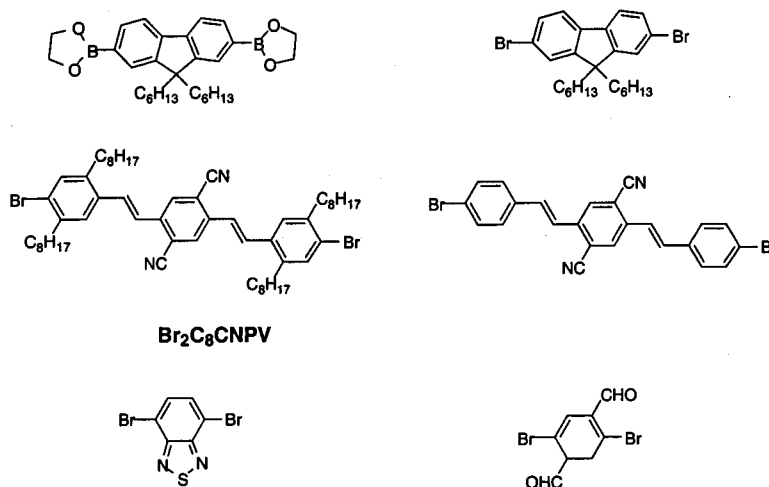
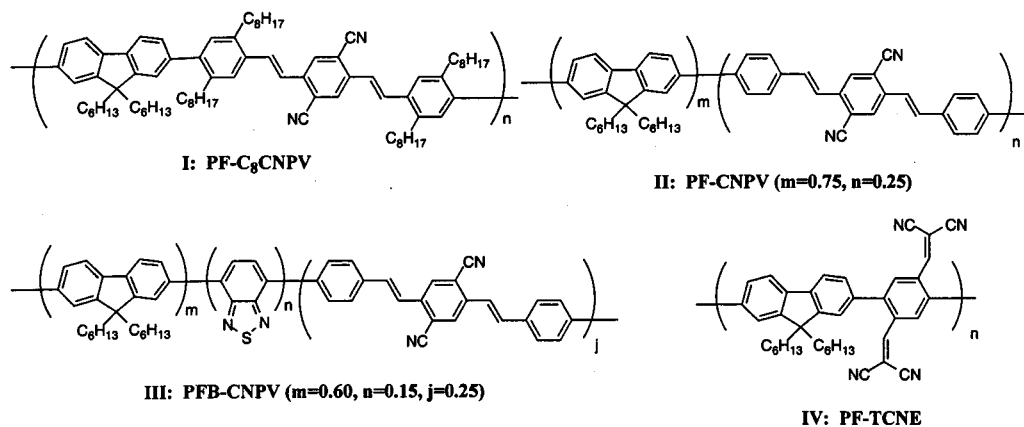


Chart 2. Fluorene Boronic Ester, Aryl Dibromide Monomers, and Copolymers Formed by the Suzuki Coupling Reaction

a. Monomers



b. Copolymers



General Procedure for Wittig–Horner Reaction. To a solution of 1:2.1 equiv of a 2,5-dicyano-*p*-xylyl-bis(diethylphosphonate) and the derivatives of benzaldehyde in THF was

added potassium *tert*-butoxide (2.1 equiv) at 0 °C. After stirring at room temperature for 2 h, the reaction was quenched with water. After the solvent was evaporated under vacuum, the

crude product was extracted from water with CH_2Cl_2 and then purified by column chromatography and crystallization.

1,4-Bis(4-*tert*-butylstyryl)benzene (1). The general procedure described above was followed using *p*-xylyl-bis(diethylphosphonate) (378 mg, 1 mmol) and 4-*tert*-butylbenzaldehyde (0.35 mL, 2.1 mmol) in the presence of tBuOK (235 mg, 2.1 mmol). After column separation, the product was recrystallized from acetone/ethanol to afford a pale yellow solid. Yield: 240 mg (60%). $^1\text{H NMR}$ (300 MHz, CDCl_3): δ 1.34 (s, 18H), 7.06 (d, $J = 15.6$ Hz, 2H), 7.13 (d, $J = 15.9$ Hz, 2H), 7.39 (dd, $J = 6.6$ Hz, 1.9 Hz, 4H), 7.47 (dd, $J = 6.6$ Hz, 1.8 Hz, 4H), 7.50 (s, 4H). $^{13}\text{C NMR}$ (CDCl_3): δ 151.55, 137.47, 135.34, 129.02, 128.31, 127.45, 126.98, 126.37, 35.38, 32.03. Anal. Calcd for $\text{C}_{30}\text{H}_{34}$: C, 91.32; H, 8.68. Found: C, 91.48; H, 8.70.

1,4-Bis(4-*tert*-butylstyryl)-2,5-dicyanobenzene (3). The general procedure described above was followed using 2,5-dicyano-*p*-xylyl-bis(diethylphosphonate) (428 mg, 1 mmol) and 4-*tert*-butylbenzaldehyde (0.35 mL, 2.1 mmol) in the presence of tBuOK (236 mg, 2.1 mmol). After column separation, the product was then recrystallized from acetone/ethanol to afford a yellow solid. Yield: 380 mg (85%). $^1\text{H NMR}$ (300 MHz, CDCl_3): δ 1.35 (s, 18H), 7.36 (d, $J = 15.6$ Hz, 4H), 7.44 (d, $J = 8.7$ Hz, 4H), 7.54 (dd, $J = 8.4$ Hz, 1.8 Hz, 4H), 8.04 (s, 2H). $^{13}\text{C NMR}$ (CDCl_3): δ 153.75, 139.71, 135.68, 133.52, 130.37, 127.95, 126.71, 121.76, 117.38, 115.71, 35.59, 31.95. Anal. Calcd for $\text{C}_{32}\text{H}_{32}\text{N}_2$: C, 86.45; H, 7.25; N, 6.30. Found: C, 86.43; H, 7.24; N, 6.53.

1,4-Bis(4-cyanostyryl)-2,5-dicyanobenzene (4). The general procedure described above was followed using 2,5-dicyano-*p*-xylyl-bis(diethylphosphonate) (428 mg, 1 mmol) and 4-cyanobenzaldehyde (262.3 mg, 2 mmol) in the presence of tBuOK (236 mg, 2.1 mmol). The yellow solid was precipitated out from THF during reaction. The solid was filtered and then rinsed with water, methanol, methylene chloride, and acetone sequentially to get rid of all the starting materials. Yield: 333 mg (87%). Anal. Calcd for $\text{C}_{26}\text{H}_{14}\text{N}_4$: C, 81.66; H, 3.69; N, 14.65. Found: C, 81.44; H, 3.89; N, 14.37.

4,4'-Di-*tert*-butyl-1,4-bis(b-cyanostyryl)benzene (2). 1,4-Phenylenediacetonitrile (156 mg, 1 mmol) and 4-*tert*-butylbenzaldehyde (0.35 mL, 2.1 mmol) were dissolved in a mixture of *tert*-butyl alcohol (9 mL) and THF (3 mL). tBuOK (11 mg, 0.1 mmol) and tetra-*n*-butylammonium hydroxide (1 mL, 1 mmol) were added quickly. The temperature was increased to 50 °C. After stirring 15 min at this temperature, the reaction mixture was poured into acidified methanol. The yellow precipitate was filtered and washed with methanol three times. The product was then recrystallized from ethanol to obtain a pale yellow solid. Yield: 111 mg (25%). $^1\text{H NMR}$ (300 MHz, CDCl_3): δ 1.36 (s, 18H), 7.51 (dd, $J = 6.9$ Hz, 2.0 Hz, 4H), 7.59 (s, 2H), 7.75 (s, 4H), 7.88 (dd, $J = 6.3$ Hz, 2.1 Hz, 4H). $^{13}\text{C NMR}$ (CDCl_3): δ 155.38, 143.35, 135.92, 131.51, 130.20, 127.50, 127.18, 126.78, 118.69, 35.80, 31.86. Anal. Calcd for $\text{C}_{32}\text{H}_{32}\text{N}_2$: C, 86.45; H, 7.25; N, 6.30. Found: C, 86.21; H, 7.08; N, 6.05.

1,4-Di(4-*tert*-butylstyryl)-2-carbonyl-5-cyanobenzene (3-CHO). To an ice-cooled suspension of **3** (155 mg, 0.35 mmol) in ether (20 mL) was added diisobutylaluminum hydride (DIBAL) (0.07 mL, 0.39 mmol) gradually. The mixture was stirred at room temperature overnight. The ice-cooled reaction mixture was then quenched carefully with methanol (0.5 mL), followed by water (1 mL) and 2 M hydrochloric acid (5 mL). Finally, concentrated HCl was added until the white solid was completely dissolved. The aqueous layer was separated and extracted twice with ether. The combined organic layers were washed successively with water, saturated NaHCO_3 solution and water, and then dried over Na_2SO_4 . After removal of the solvent, the crude product was purified by a silica gel column using hexane/ CH_2Cl_2 (7:3) as eluent. Yield: 47 mg (30%). $^1\text{H NMR}$ (300 MHz, CDCl_3): δ 1.35 (s, 18H), 7.19 (d, $J = 16.2$ Hz, 2H), 7.43 (dd, $J = 8.7$ Hz, 3.9 Hz, 4H), 7.54 (dd, $J = 8.4$ Hz, 4.2 Hz, 4H), 7.97 (d, $J = 16.2$ Hz, 2H), 8.19 (s, 1H), 8.24 (s, 1H), 10.46 (s, 1H). Anal. Calcd for $\text{C}_{32}\text{H}_{33}\text{NO}$: C, 85.87; H, 7.43; N, 3.13. Found: C, 86.11; H, 7.28; N, 3.05.

1,4-Di(4-*tert*-butylstyryl)-2-cyano-5-dicyanovinylbenzene (5). To a solution of **3-CHO** (58 mg, 0.13 mmol) and

malononitrile (88 mg, 1.3 mmol) in chloroform (20 mL) was added pyridine (3–4 drops). The mixture was refluxed under nitrogen for 24 h. The product was extracted from water with CH_2Cl_2 and purified by a silica gel column using hexane/ CH_2Cl_2 (1:1) as eluent. The crude product was recrystallized from acetone/ethanol to afford an orange solid. Yield: 58 mg (90%). $^1\text{H NMR}$ (300 MHz, CDCl_3): δ 1.35 (s, 18H), 6.97 (d, $J = 15.6$ Hz, 2H), 7.08 (d, $J = 15.6$ Hz, 2H), 7.43 (dd, $J = 8.7$ Hz, 3.9 Hz, 4H), 7.54 (dd, $J = 8.4$ Hz, 4.2 Hz, 4H), 7.92 (s, 1H), 8.19 (s, 1H), 8.35 (s, 1H). $^{13}\text{C NMR}$ (CDCl_3): δ 158.20, 153.96, 140.26, 138.22, 136.10, 133.55, 132.66, 128.03, 127.83, 126.66, 126.03, 122.26, 117.54, 115.71, 112.61, 35.59, 31.95. Anal. Calcd for $\text{C}_{35}\text{H}_{33}\text{N}_3$: C, 84.81; H, 6.71; N, 8.48. Found: C, 84.92; H, 6.76; N, 8.66.

1,4-Di(4-*tert*-butylstyryl)-2,5-dicarbonylbenzene (3-di-CHO). Compound **3-diCHO** was synthesized following the same procedure for **3-CHO** using **3** (222 mg, 0.5 mmol) and DIBAL (0.3 mL, 1.7 mmol). Yield: 113 mg (50%). $^1\text{H NMR}$ (300 MHz, CDCl_3): δ 1.35 (s, 18H), 7.19 (d, $J = 16.2$ Hz, 2H), 7.43 (dd, $J = 8.4$ Hz, 1.8 Hz, 4H), 7.54 (d, $J = 8.4$ Hz, 4H), 7.97 (d, $J = 16.2$ Hz, 2H), 8.18 (s, 2H), 10.45 (s, 2H). Anal. Calcd for $\text{C}_{32}\text{H}_{34}\text{O}_2$: C, 85.29; H, 7.60. Found: C, 85.41; H, 7.44.

1,4-Di(4-*tert*-butylstyryl)-2,5-bis(dicyanovinyl)benzene (6). Compound **6** was synthesized following the same procedure for **5** using **3-diCHO** (80 mg, 0.18 mmol) and malononitrile (17 mg, 1.8 mmol). Yield: 81 mg (84%). $^1\text{H NMR}$ (300 MHz, CDCl_3): δ 1.35 (s, 18H), 7.00 (d, $J = 16.2$ Hz, 2H), 7.15 (d, $J = 15.6$ Hz, 2H), 7.46 (dd, $J = 8.4$ Hz, 3.9 Hz, 4H), 7.52 (dd, $J = 8.7$ Hz, 3.9 Hz, 4H), 8.20 (s, 2H), 8.24 (s, 2H). $^{13}\text{C NMR}$ (CDCl_3): δ 157.49, 150.74, 138.72, 138.30, 133.11, 132.51, 128.13, 127.41, 126.25, 121.52, 113.17, 112.24, 35.11, 31.44. Anal. Calcd for $\text{C}_{38}\text{H}_{34}\text{N}_4$: C, 83.48; H, 6.27; N, 10.25. Found: C, 83.37; H, 6.20; N, 10.16.

$\text{Br}_2\text{C}_8\text{CNPV}$. The general procedure for the Wittig–Horner reaction was followed using 2,5-dicyano-*p*-xylyl-bis(diethylphosphonate) (428 mg, 1 mmol) and 4-bromo-2,5-di-*n*-octylbenzaldehyde (819 mg, 2 mmol) in the presence of tBuOK (235.7 mg, 2.1 mmol). Yield: 486 mg (52%). $^1\text{H NMR}$ (300 MHz, CDCl_3): δ 0.86 (t, $J = 6.2$ Hz, 12H), 1.285 (br, 48H), 2.70 (q, $J = 7.8$ Hz, 8H), 7.24 (d, $J = 16.2$ Hz, 2H), 7.39 (s, 2H), 7.45 (s, 2H), 7.52 (d, $J = 16.2$ Hz, 2H), 8.00 (s, 2H). Anal. Calcd for $\text{C}_{56}\text{H}_{78}\text{Br}_2\text{N}_2$: C, 71.63; H, 8.37; Br, 7.02; N, 2.98. Found: C, 71.46; H, 8.55; Br, 6.89; N, 3.04.

General Procedure for the Suzuki Coupling Polymerization. To a stirred mixture of the 9,9-dihexylfluorene-2,7-di(ethylenyl boronate) (1 equiv), aryl dibromide (1.05 equiv), tetrakis(triphenylphosphine)palladium (1 wt %), and Aliquat 336 (tricaprylylmethylammonium chloride 10 wt %, purchased from Aldrich Chemical) in toluene (10 mL) under nitrogen was added a 2 M aqueous potassium carbonate solution (3.3 equiv). The mixture was heated to reflux for 3 days. The polymerization was end-capped with phenylboronic acid for 6 h, followed by bromobenzene for another 6 h. The reaction mixture was cooled and added dropwise into a methanol/water (2:1 v/v) solution. The precipitated polymer fibers were collected by filtration. The crude polymer was further purified by redissolving the polymer into THF and reprecipitating in methanol several times.

$\text{PF-C}_8\text{CNPV}$. The general procedure described above was followed using 9,9-dihexylfluorene-2,7-di(ethylenyl boronate) (190 mg, 0.4 mmol) and $\text{Br}_2\text{C}_8\text{CNPV}$ (394 mg, 0.42 mmol) in the presence of tetrakis(triphenylphosphine)palladium (1.9 mg), Aliquat 336 (19 mg), and 2 M K_2CO_3 (0.6 mL). Yield: 355 mg (80%). $^1\text{H NMR}$ (300 MHz, CDCl_3): δ 0.77 (t, $J = 6.6$ Hz, 6H), 0.87 (t, $J = 7.2$ Hz, 12H), 1.08–1.28 (m, 64H), 2.68 (br, 4H), 2.82 (br, 8H), 7.18 (br, 4H), 7.33–7.51 (m, 6H), 7.61–7.81 (m, 4H), 8.08 (s, 2H). Anal. Calcd for $(\text{C}_{81}\text{H}_{110}\text{N}_2)_n$: C, 87.51; H, 9.97; N, 2.52. Found: C, 88.31; H, 9.52; N, 2.14.

PF-CNPV . The general procedure described above was followed using 9,9-dihexylfluorene-2,7-di(ethylenyl boronate) (181 mg, 0.38 mmol), 9,9-dihexylfluorene-2,7-dibromide (98 mg, 0.2 mmol), and 1,4-bis(4-bromostyryl)-2,5-dicyanobenzene (98 mg, 0.2 mmol) in the presence of tetrakis(triphenylphosphine)palladium (2 mg), Aliquat 336 (18 mg), and 2 M K_2CO_3 (0.6 mL). Yield: 257 mg (51%). $^1\text{H NMR}$ (300 MHz, CDCl_3): δ 0.80

(br, 18H), 1.15 (br, 48H), 2.11 (br, 12H), 7.45 (br, 4H), 7.69–7.85 (m, 26H), 8.14 (br, 2 H). Anal. Calcd for $(C_{99}H_{110}N_2)_n$: C, 89.54; H, 8.35; N, 2.11. Found: C, 90.15; H, 8.02; N, 1.68.

PFB–CNPV. The general procedure described above was followed using 9,9-dihexylfluorene-2,7-di(ethylenyl boronate) (181 mg, 0.38 mmol), 9,9-dihexylfluorene-2,7-dibromide (39 mg, 0.08 mmol), 4,7-dibromo-2,1,3-benzothiadiazole (35 mg, 0.12 mmol), and 1,4-bis(4-bromostyryl)-2,5-dicyanobenzene (98 mg, 0.2 mmol) in the presence of tetrakis(triphenylphosphine)palladium (2 mg), Aliquat 336 (18 mg), and 2 M K_2CO_3 (0.6 mL). Yield: 163 mg (86%). 1H NMR (300 MHz, $CDCl_3$): δ 0.79 (br, 24H), 1.15 (br, 64H), 2.19 (br, 16H), 7.45 (br, 6.67H), 7.68–8.13 (m, 42.66H). Anal. Calcd for $(C_{146}H_{153.33}N_{5.33}Si)_n$: C, 87.03; H, 7.67; N, 3.71. Found: C, 87.90; H, 7.25; N, 4.05.

PF–TCNE. The general procedure described above was followed using 9,9-dihexylfluorene-2,7-di(ethylenyl boronate) (237 mg, 0.5 mmol) and 2,5-dibromoterephthalaldehyde (153 mg, 0.525 mmol) in the presence of tetrakis(triphenylphosphine)palladium (2.4 mg), Aliquat 336 (24 mg), and 2 M K_2CO_3 (0.8 mL). Yield: 193 mg (83%). 1H NMR (300 MHz, $CDCl_3$): δ 0.79 (t, $J = 6.6$ Hz, 6H), 1.12 (br, 16H), 2.07 (t, $J = 6.3$ Hz, 4H), 7.41–7.96 (m, 6H), 8.08 (s, 1H), 8.26 (s, 1H), 10.11 (s, 1 H), 10.16 (s, 1H). **PF–TCNE** was formed by the further condensation of above prepolymer (100 mg, 0.2 mmol) with malononitrile (132 mg, 2 mmol). Yield: 36 mg (33%). 1H NMR (300 MHz, $CDCl_3$): δ 0.79 (t, $J = 6.3$ Hz, 6H), 1.13 (br, 16H), 2.08 (t, $J = 6.6$ Hz, 4H), 7.44–7.98 (m, 6H), 8.09 (s, 1H), 8.22 (s, 1H), 8.44 (s, 2 H). Anal. Calcd for $(C_{39}H_{36}N_4)_n$: C, 83.53; H, 6.47; N, 10.00. Found: C, 83.02; H, 7.02; N, 8.94.

General Characterization Methods. 1H and ^{13}C NMR spectra were obtained on a Bruker AF300 (300 MHz) spectrometer and recorded in ppm relative to tetramethylsilane (TMS) ($\delta = 0$ ppm) as an internal standard. Molecular weights of the polymers were determined by gel permeation chromatography (GPC) on a Waters Styragel (HR 4E, 7.8×300 mm) column with polystyrenes as the standards and THF as the solvent. Thermal properties of polymers were analyzed with a TA Instruments thermal analysis and rheology system (TGA 2950, DSC 2010) under nitrogen at a heating rate of 10 °C/min. UV–vis spectra were recorded on a Perkin-Elmer spectrophotometer (Lambda 9 UV/vis/NIR). The film thickness was measured with a Dektak surface profilometer (model 3030). Photoluminescence (PL) efficiencies of the neat films (cast on quartz glass) were recorded on an Oriel Instaspec IV charge coupled device (CCD) camera and a Newport integrating sphere.¹⁹ EL spectra of LEDs were obtained with the same CCD system. Current–voltage (I – V) and luminance–voltage (L – V) characteristics were measured on a Hewlett-Packard 4155B semiconductor parameter analyzer together with a Newport 2835-C multifunctional optical meter. Photometric units (cd/m^2) were calculated using the forward output power and the EL spectra of the devices, assuming Lambertian distribution of the EL emission.²⁰

Cyclic voltammetry (CV) was conducted at room temperature in a typical three-electrode cell with a working electrode (ITO glass), a reference electrode (Ag/Ag^+ , referenced against ferrocene/ferrocenium (FOC), 0.12 V), and a counter electrode (Pt gauze) under a nitrogen atmosphere at a sweeping rate of 100 mV/s (CV-50W voltammetric analyzer, BAS). CV measurements for oligomers were performed in an electrolyte solution of 0.1 M tetrabutylammonium hexafluorophosphate (Bu_4NPF_6) in 1,2-dichloroethane (DCE), while a solution of 0.1 M tetrabutylammonium perchlorate (TBAP) in acetonitrile was used as the electrolyte for polymer films.

LEDs Fabrication. The EL devices were constructed using a double-layer configuration with an in-situ polymerized bis(tetraphenyldiamino)biphenyl–perfluorocyclobutane (BTPD–PFCB) as the hole-transporting layer^{21,22} and the cyano-containing polymers as the emitting layer. The BTPD–PFCB layer was first spin-coated from its DCE solution (1 wt %) onto ITO glass substrates and then cured at 225 °C for 1 h. Then a thin layer of light-emitting polymers (1 wt % in DCE) was spin-coated onto the BTPD–PFCB layer. A layer of 30 nm thick Ca was vacuum-deposited at pressure below 10^{-6} Torr through a mask, and another layer of 120 nm thick Ag was

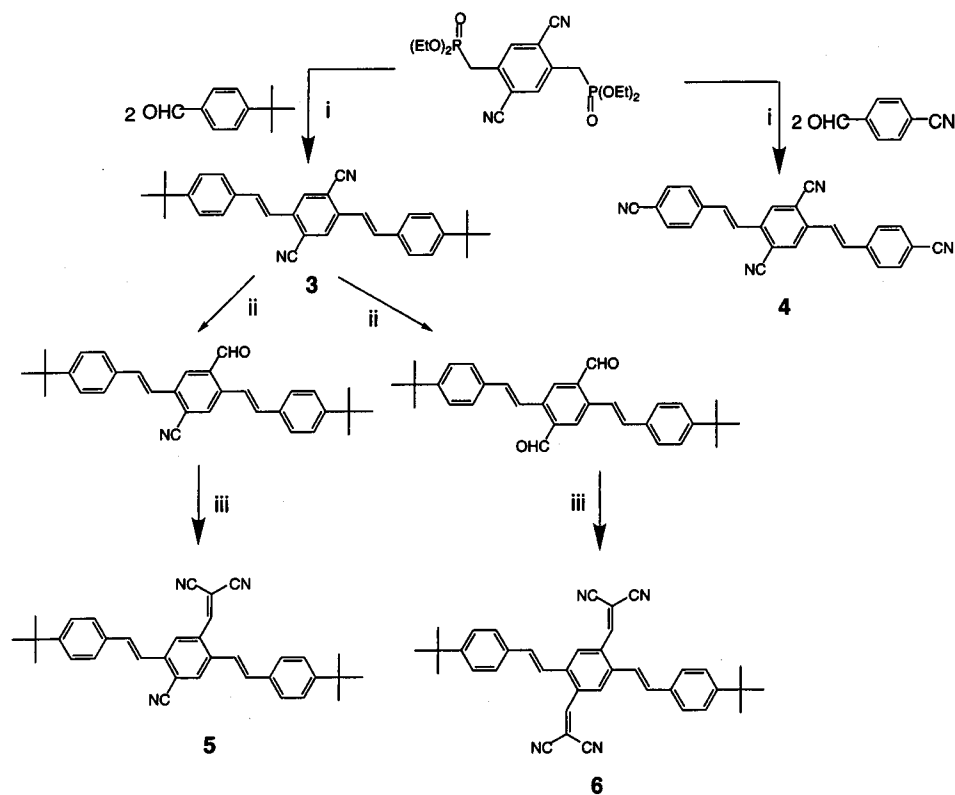
vacuum-deposited on the top as a protecting layer for Ca. The active emissive area defined by the cathode was about 8 mm². The “electron-only” devices were prepared as a sandwich structure between Al and Ca electrodes.

Results and Discussion

Synthesis. Chart 1 presents a series of cyano-containing compounds **3–6**, which are arranged according to the increasing strength of electron-withdrawing substituents. Compounds **3** and **4** were synthesized by the Wittig–Horner condensation reaction between 1,4-bis(2,5-dicyanobenzal phosphonate) and 4-*tert*-butylbenzaldehyde and 4-cyanobenzaldehyde, respectively (Scheme 1). Further chemical reduction of the cyano groups on compound **3** by diisobutylaluminum hydride (DIBAL) afforded a monoaldehyde and a dialdehyde depending on the stoichiometric ratios between **3** and DIBAL. Condensation of the resulting aldehydes with malononitrile gave compounds **5** and **6** in almost quantitative yield. The unsubstituted compound **1** and the cyanoterephthalylidene **2** were also synthesized for comparison (Chart 1). Compound **4** is insoluble in common organic solvent, such as THF, chloroform, and DCE, due to its symmetrical and rigid structure. However, the result obtained from elemental analysis verified the composition of the desired compound. Compounds **1–3**, **5**, and **6** could be purified by recrystallization from acetone/ethanol after brief purification through column chromatography. The stereochemistry of the expected trans olefinic linkage was verified by the coupling constant of the vinylene protons in 1H NMR ($J = 15$ – 17 Hz).

Suzuki coupling methodology was employed in the polymerization since it is tolerant of a large variety of functional groups, insensitive to the presence of water, and easy to make high molecular weight polymers.²³ Polymers **I–III** were synthesized by coupling fluorene diboronic esters with various cyano-containing distyrylbenzene dibromides and benzothiadiazole dibromide in the presence of Pd complex catalyst (Chart 2). While the polycondensation of fluorene diboronic ester with 2,5-dibromoterephthalic dialdehyde gave polyaldehyde initially, PF–TCNE (**IV**) was obtained by a further condensation reaction of the resulting prepolymer with malononitrile. The structures of the monomers and polymers were confirmed by 1H NMR and elemental analysis. The polymer compositions were estimated from the feeding ratio. All the polymers could be very easily dissolved in common organic solvents, such as chloroform, THF, and DCE. The weight-average molecular weights (M_w) of these polymers determined by gel permeation chromatography (GPC) range from 27 700 to 148 500 with polydispersity ranging from 1.7 to 3.3 using polystyrenes as the standards (Table 1). Thermal characterization of polymers was accomplished by thermogravimetry analysis (TGA) and differential scanning calorimetry (DSC). The corresponding data are summarized in Table 1. All the polymers except PF–TCNE show excellent thermal stability with decomposition temperature (onset of weight loss, measured by TGA analysis, 10 °C/min) in excess of 380 °C. PF–TCNE undergoes a two-step weight loss: at 224 °C, it starts to lose dicyanovinyl substituents, while decomposition temperature of polymer main chain is at 382 °C. These polymers also exhibit relatively high T_g 's, ranging from 141 to 174 °C.

Electrochemical and Charge Transport Properties. Table 2 lists the values of onset redox potentials

Scheme 1. Synthetic Route for the Cyano-Containing Distyrylbenzenes^a

^a Reagents and conditions: (i) ^tBuOK, THF, 2 h; (ii) DIBAL, ether, 0 °C; (iii) malononitrile, pyridine, CHCl₃, reflux, 24 h.

Table 1. Characteristics of the Cyano-Containing Copolymers

copolymer	M_w	M_w/M_n	T_g (°C)	T_d (°C)
PF-C ₈ CNPV	51 100	2.83	174	389
PF-CNPV	64 000	3.12	141	379
PFB-CNPV	148 000	3.29	149	406
PF-TCNE	27 700	1.68	163	224, 382

Table 2. Redox Properties of the Distyrylbenzenes

model compd	E^{ox} (V) ^a	E^{red} (V) ^a	HOMO (eV) ²⁴	LUMO (eV) ²⁴
1	1.04		-5.72	
2		-1.52		-3.16
3		-1.46		-3.22
4		-1.40 ^b		-3.28
5		-0.87		-3.81
6		-0.67		-4.01

^a Onset potentials vs Ag/Ag⁺. ^b Thin film evaporated onto ITO.

of the model compounds from electrochemical study. The unsubstituted parent compound **1** exhibits two reversible oxidative waves (Figure 1), corresponding to the successive generation of the cation radical and dication. No reduction is observed for this molecule under the experimental conditions. However, the addition of the cyano or dicyanovinyl functional groups enhances the electron affinity of compounds significantly; only reduction processes could be observed for the cyano-containing compounds. Their electron affinities increase with the increasing electron-withdrawing strength of the acceptors. Moreover, the position of electron-withdrawing functional groups also affects the stability of the anion radical. Figure 1 shows the cyclic voltammograms of compounds **2** and **3**. The onset and reduction peak potentials of **3** are nearly identical to those of **2**, indicating that different positions of the cyano substitution have a similar influence on electron affinity of the

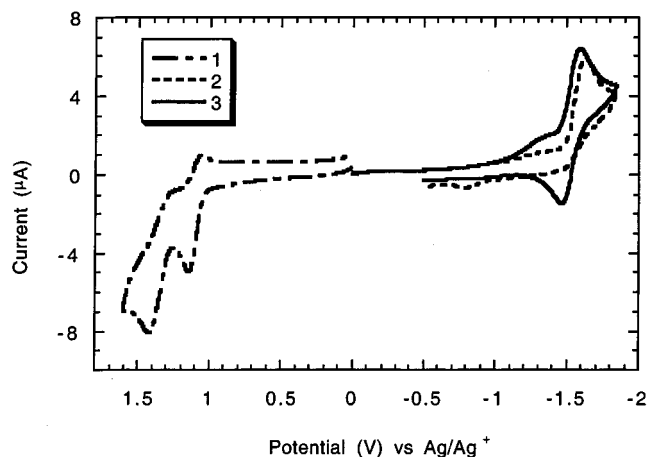


Figure 1. Cyclic voltammograms of the electrochemical oxidation of compound **1** and reduction of compounds **2** and **3** in 0.1 M TBAPF₆ in DCE at a sweep rate of 100 mV/s.

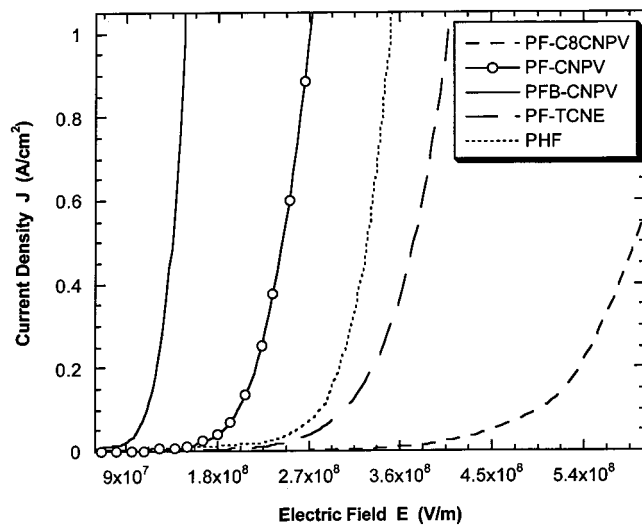
carbon framework. They possess comparable electron affinity. However, compound **3** shows a distinct, reversible wave, while only an irreversible wave is observed for compound **2**. The reversible reduction wave of **3** can be cycled repetitively without any appreciable change. This can be explained that the vinylenic nitrile (an α,β -unsaturated system) is very susceptible to attack from nucleophiles. As a result, it breaks the conjugation and electroactivity of the molecule. The improved stability of radical anions through these cyano groups on the aromatic ring may eventually contribute to the durability of the LED devices.

As was expected, by attaching a stronger electron-accepting dicyanovinyl group onto the phenylene, it can further improve the electron affinity of the parent compound. Compound **6** demonstrates a much lower

Table 3. Physical Properties of the Cyano-Containing Copolymers

copolymer	λ_{UV} (nm) ^a	HOMO (eV) ^b	LUMO (eV) ^c	λ_{PL} (nm) ^d	PL efficiency (%)
PF-C ₈ CNPV	408	-5.75	-3.12	504	17
PF-CNPV	380, 432	-5.93	-3.43	513	15
PFB-CNPV	345, 447	-5.76	-3.22	541	10
PF-TCNE	326	-6.33	-4.00	616	4

^a Maximum wavelength of absorption (film). ^b From absorption spectra. ^c From cyclic voltammetry data. ^d Maximum wavelength of emission (film), excited at absorption maximum.

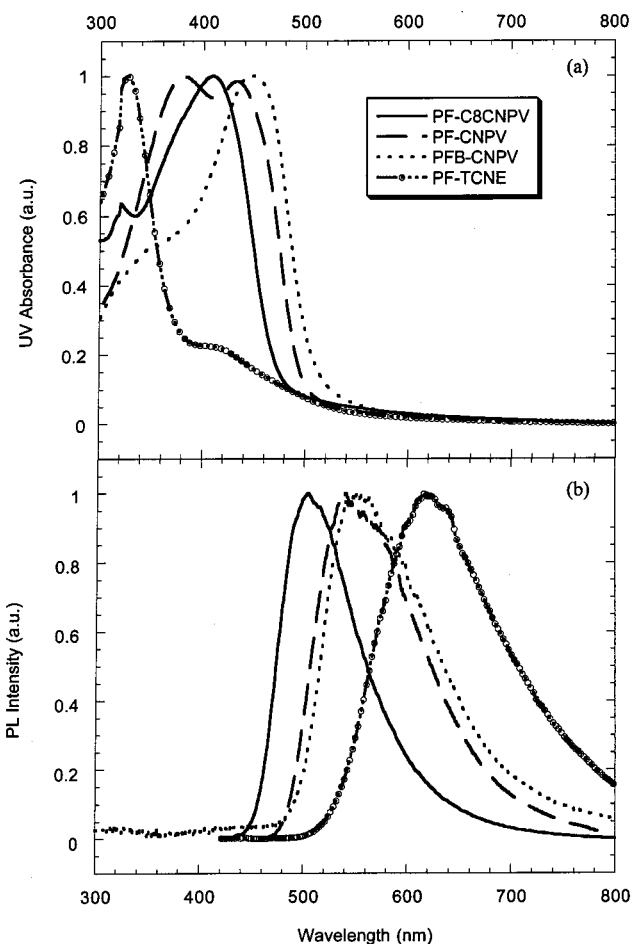
**Figure 2.** Current density–electric field characteristics of “electron-only” devices.

reduction onset at -0.67 V, which indicates easier accessible radical anions (Table 2).

Our model study demonstrates that the incorporation of cyano functional groups onto the phenylene ring not only enhances electron affinity but also increases anion stability. Thus, the monomers bearing cyano-containing distyrylbenzenes were used to copolymerize with fluorene to improve electron-transporting properties of polyfluorenes.

As we compare the data of the LUMO level obtained from cyclic voltammetry (CV),²⁴ it shows that the LUMO levels of the polymers are similar to those of their oligomeric model compounds, indicating improved electron affinity of these cyano-containing polymers (Table 3).

The electron-transporting properties were investigated using an “electron-only” devices consisting of a polymer layer sandwiched between Al and Ca electrodes.²⁵ By replacing the high work function ITO (4.7 eV) with a lower work function metal Al (4.3 eV), it increases the energy barrier for hole injection. This will reduce the number of injected holes to the HOMO level of the polymers. In addition, there is no energy barrier for electron injection due to low LUMO levels of these cyano-containing polymers. Therefore, the current density–electric field (J – E) characteristics are only related to the bulk electron conduction of polymer films. A single-carrier device using fluorene homopolymer, poly-(9,9-dihexylfluorene) (PHF), as the active layer was also fabricated for comparison. The J – E characteristics of these testing devices demonstrate that the best electron conduction is achieved in the PFB–CNPV system (Figure 2). At the same electric field, the electron current density of the PFB–CNPV device is the highest

**Figure 3.** Optical absorption (a) and photoluminescence (b) spectra of thin films of cyano-containing polymers.

among all devices. This may be due to the better planarity of benzothiadiazole that provides a better electron-hopping manifold. The presence of alkyl chains on PF–C₈CNPV improves the solubility and decreases chain packing of the polymer. However, it significantly hinders the electron conduction. Thus, the polymer suffers from the slowest electron motion. On the other hand, PF–TCNE possesses the highest electron affinity, but its electron motion is relatively slow. This is understandable because the dicyanovinyl group is a very strong electron acceptor, and it may act as a deep trap site for electrons in the bulk film. From these studies, the PFB–CNPV shows a combined high electron affinity and conductivity that makes it an ideal candidate as a good electron-transporting material.

Photophysical Properties. The UV–vis absorption and emission spectra of the copolymers are shown in Figure 3, and the results are summarized in Table 3. The longer absorption wavelength of PFB–CNPV compared with that of other copolymers further confirms its more planar structure. When the strong electron-withdrawing dicyanovinyl groups were introduced into the polymer main chain, a higher energy absorption peak at 326 nm with a broad shoulder at 410 nm was observed.

All the polymers possess broad, featureless emission bands. The emission maximum of the PF–C₈CNPV with octyl substitutions on the distyrylbenzene is at 504 nm, which is blue-shifted compared to those polymers without octyl chains (PF–CNPV and PFB–CNPV) because of backbone distortion induced by the alkyl chains. PF–

Table 4. Performance of LEDs Based on Cyano-Containing Copolymers

device configuration	d (nm) ^a	V_{on} (V) ^b	B_{max} (cd/m ²) ^c	η_{max} (%) ^d
ITO/BTPD–PFCB/PF–C ₈ CNPV/Ag	55	6.0	1220	0.53
ITO/BTPD–PFCB/PF–CNPV/Ag	50	3.6	837	0.07
ITO/BTPD–PFCB/PFB–CNPV/Ag	55	4.4	2050	0.32
ITO/BTPD–PFCB/PF–TCNE/Ag	40	13.2	36	0.02
ITO/BTPD–PFCB/PFB–CNPV/Ca	60	2.6	4730	0.88

^a Thickness of the emitting layer. ^b Turn-on voltage, defined as the voltage required to give a luminance of 1 cd/m². ^c Maximum brightness. ^d Maximum external quantum efficiency.

C₈CNPV also possesses higher photoluminescence (PL) efficiency. This may be due to the presence of the octyl substitutions decreasing intermolecular packing and thus reducing luminescence quenching. The emission of PF–TCNE has a significant red shift relative to the rest of polymers, in which a very low PL quantum yield, 4%, was obtained. This may be caused by the intramolecular charge transfer (ICT) between the fluorene and the bis(dicyanovinyl)benzene ring. ICT is much stronger in the PF–TCNE than the other cyano-containing polymers (**I**–**III**) since the dicyanovinyl group is a much stronger electron acceptor.

Electroluminescence. EL of single-layer devices made from the cyano-containing polymers using the ITO/polymer/Ag configuration ($\phi_{\text{Ag}} \sim 4.3$ eV) showed very poor performance with very high turn-on voltage (> 13 V) and low brightness due to large energy barriers for both electron and hole injection. By employing a hole-transporting layer (BTPD–PFCB), good EL efficiency and luminance were achieved in the devices with the configuration of ITO/HTL/polymer/Ag (Table 4). Although the PF–C₈CNPV-based device has the highest efficiency, the brightness is very low due to much slower electron motion. The ITO/BTPD–PFCB/PFB–CNPV/Ag device has the best overall performance, with a turn-on voltage of 4.4 V and a luminance of 2050 cd/m² at 0.68 A/cm². This could be attributed to both optimized carrier injection and electron conduction in this configuration. For the polymers with similar structure (**I**–**III**), the turn-on voltage increases with the increasing energy barrier for the electron injection, which indicates that the device performance is still limited by electron injection from the silver electrode, since there is still a quite large energy barrier (~ 1 eV) between Ag and the polymers. This is confirmed by a device fabricated using another bilayer configuration (ITO/BTPD–PFCB/PFB–CNPV/Ca) with a low work function calcium metal as the cathode. The ohmic contact between PFB–CNPV (LUMO ~ 3.3 eV) and calcium ($\phi_{\text{Ca}} \sim 2.9$ eV) greatly facilitates the electron injection. The device can be turned on at 2.6 V, and it reached a high luminance of 4730 cd/m² at a current density of 1.62 A/cm². The external quantum efficiency of the device also improves by approximately a factor of 3 ($\eta_{\text{EL}} = 0.88\%$).

Summary

A series of cyano-containing distyrylbenzenes were synthesized as model compounds to systematically study

the effect of cyano substituents on the redox behaviors of conjugated molecules. The results derived from the structure/property relationships among these compounds enabled us to design and synthesize a new class of fluorene-based copolymers with these cyano-containing chromophores as comonomers to improve the electron affinities and transport of these light-emitting materials.

Acknowledgment. The authors thank the Air Force Office of Scientific Research (AFOSR) for support through the MURI (Polymeric Smart Skins) and the DURIP program. A. Jen thanks the Boeing-Johnson Foundation for financial support. M. Liu thanks the Nanotechnology Center at the University of Washington for the nanotechnology fellowship.

References and Notes

- (1) Kraft, A.; Grimsdale, A. C.; Holmes, A. B. *Angew. Chem., Int. Ed.* **1998**, *37*, 402.
- (2) Friend, R. H.; Gymer, R. W.; Holmes, A. B.; Burroughes, J. H.; Marks, R. N.; Taliani, C.; Bradley, D. D. C.; Dos Santos, D. A.; Brédas, J. L.; Lögdlund, M.; Salaneck, W. R. *Nature (London)* **1999**, *397*, 121.
- (3) Bernius, M. T.; Inbasekaran, M.; O'Brien, J.; Wu, W. W. *Adv. Mater.* **2000**, *12*, 1737.
- (4) Lyon, L. *Mol. Cryst. Liq. Cryst.* **1989**, *171*, 53.
- (5) Bradley, D. D. C. *Synth. Met.* **1993**, *54*, 401.
- (6) Martens, H. C. F.; Huijberts, J. N.; Blom, P. W. M. *Appl. Phys. Lett.* **2000**, *77*, 1852.
- (7) Blom, P. W. M.; de Jong, M. J. M.; Vleggaar, J. J. M. *Appl. Phys. Lett.* **1996**, *68*, 3308.
- (8) Renak, M. L.; Bartholomew, G. P.; Wang, S.; Ricatto, P. J.; Lachicotte, R. J.; Bazan, G. C. *J. Am. Chem. Soc.* **1999**, *121*, 7787.
- (9) Oelkrug, D.; Tompert, A.; Gierschner, J.; Egelhaaf, H.-J.; Hanack, M.; Hohloch, M.; Steinhuber, E. *J. Phys. Chem. B* **1998**, *102*, 1902.
- (10) Strehmel, B. A.; Sarker, M.; Malpert, J. H.; Strehmel, V.; Seifert, H.; Neckers, D. C. *J. Am. Chem. Soc.* **1999**, *121*, 1226.
- (11) Greenham, N. C.; Moratti, S. C.; Bradley, D. D. C.; Friend, R. H.; Holmes, A. B. *Science* **1993**, *365*, 628.
- (12) Rehahn, M.; Schlüter, A.-D.; Feast, W. J. *Synthesis* **1988**, 386.
- (13) Wadsworth, W. S., Jr. *Org. React.* **1977**, *25*, 73.
- (14) Inbasekaran, M.; Wu, W. W.; Wu, E. P. US Patent 5,777,070, 1998. Inbasekaran, M.; Wu, E. P.; Wu, W. W.; Bernius, M. T. International Patent WO 00/46321, 2000.
- (15) Shimura, Y.; Kawai, T.; Minegishi, T. *Synthesis* **1993**, 43.
- (16) Brizius, G.; Pschirer, N. G.; Steffen, W.; Stitzer, K.; zur Loye, H.-C.; Bunz, U. H. F. *J. Am. Chem. Soc.* **2000**, *122*, 12435.
- (17) Pilgram, K.; Zupan, M.; Skiles, R. *J. Heterocycl. Chem.* **1970**, *7*, 629.
- (18) Woo, E. P.; Inbasekaran, M.; Shiang, W. R.; Roof, G. R.; Bermois, M. T.; Wu, W. W. U.S. Patent 6,169,163, 1997.
- (19) Mello, J. C.; Wittmann, H. F.; Friend, R. H. *Adv. Mater.* **1997**, *9*, 230.
- (20) Greenham, N. C.; Friend, R. H.; Bradley, D. D. C. *Adv. Mater.* **1994**, *6*, 491.
- (21) Liu, S.; Jiang, X. Z.; Ma, H.; Liu, M. S.; Jen, A. K.-Y. *Macromolecules* **2000**, *33*, 3514.
- (22) Jiang, X. Z.; Liu, S.; Liu, M. S.; Ma, H.; Jen, A. K.-Y. *Appl. Phys. Lett.* **2000**, *76*, 2985.
- (23) Suzuki, A.; Miyaura, N. *Chem. Rev.* **1995**, *95*, 2457.
- (24) According to the redox onset potentials of the CV measurements, the HOMO and LUMO energy levels for the oligomers and polymers are estimated on the basis of the reference energy level of ferrocene (4.8 eV below the vacuum level): HOMO/LUMO = $-(E_{\text{onset}} - 0.12 \text{ V}) - 4.8 \text{ eV}$, where the value 0.12 V for FOC vs Ag/Ag⁺.
- (25) Parker, I. D. *J. Appl. Phys.* **1994**, *75*, 1656.

MA011790F